ELSEVIER

Journal of Hazardous Materials B135 (2006) 232–241

Journal of Hazardous Materials

www.elsevier.com/locate/jhazmat

Applicability of the various adsorption models of three dyes adsorption onto activated carbon prepared waste apricot

Canan Akmil Başar*

Inonu University, Faculty of Engineering, Department of Chemical Engineering, 44280 Malatya, Turkey

Received 14 October 2005; accepted 20 November 2005
Available online 25 January 2006

Abstract

In this study, activated carbon (WA11Zn5) was prepared from waste apricot, which is waste in apricot plants in Malatya, by chemical activation with $ZnCl_2$. BET surface area of activated carbon is determined as 1060 m^2/g. Activated carbon includes both micro and mesopores. Percentages of micropores and mesopores area are determined 36% and 74%, percentage of micropores and mesopores volume is 19% and 81%, respectively. The ability of WA11Zn5, to remove three dyes, methylene blue (MB), malachite green (MG), and crystal violet (CV), from effluent solutions by adsorption has been studied. The adsorption capacities of WA11Zn5 decreases in the order malachite green (MG) > methylene blue (MB) > crystal violet (CV). Equilibrium isotherms for the adsorption of three dyes on activated carbon were measured experimentally. Results were analyzed by the Langmiur, Freundlich, Dubinin–Redushkevich (D–R), Temkin, Frumkin, Harkins–Jura, Halsey and Henderson equation using linearized correlation coefficient at different temperature. The characteristic parameters for each isotherm have been determined. Models and the isotherm constant were evaluated depending on temperature. Langmiur and Frumkin equation is found to best represent the equilibrium data for three dye-WA11Zn5 systems.

Keywords: Dye; Adsorption; Isotherms; MG; MB; CV

1. Introduction

Activated carbon produced from environmental waste with high carbon content is the most important material to clean environmental pollution (gases and liquid impurities). Environmental wastes are very important starting material for preparing activated carbon. Various polymeric wastes, based on petroleum, agriculture by-product (ligno-cellulosic) and coals, are commonly used as a starting material for preparing activated carbon. Characteristics of importance in choosing carbon types include pore structure, particle size, total surface area and void space between particles [1]. After selection of a source, preparations for use are made. These preparations most often include dehydration, carbonization, and activation. Dehydration and carbonization involve slow heating of the source in anaerobic conditions. Chemicals such as zinc chloride or phosphoric acid can be used to enhance these processes. The stage of activation requires exposure to additional chemicals or other oxidizing agents such as a mixture of gases. Depending upon the specifics of the process and the source carbon, the newly activated carbon can be classified according to density, hardness, and other characteristics [2].

Activated carbon adsorption is an effective means for reducing organic chemicals, chlorine, lead, and unpleasant tastes and odors in effluent or colored substances from gas or liquid streams. Color removal from industrial waste-waters by adsorption techniques has been of growing importance. The chemical and biological stability of dyestuffs to conventional water treatment methods and the growing need for high quality treatment have made adsorption a very favorable treatment process. Adsorption rate and equilibrium data are the basic requirements for the design of adsorption systems. Adsorption isotherms have been studied by many researchers [3–7].

The main objects of this paper are: (i) to study the feasibility of using WA11Zn5 as an adsorbent for the removal MG, MB and CV dyes; (ii) to determine the characterization of activated carbon prepared from waste apricot; (iii) to determine the various

* Tel.: +90 422 341 0010/4445; fax: +90 422 341 0046.
E-mail address: cabasar@inonu.edu.tr.
URL: http://www.web.inonu.edu.tr/~actcarlab.

0304-3894/$ – see front matter © 2005 Elsevier B.V. All rights reserved.
doi:10.1016/j.jhazmat.2005.11.055

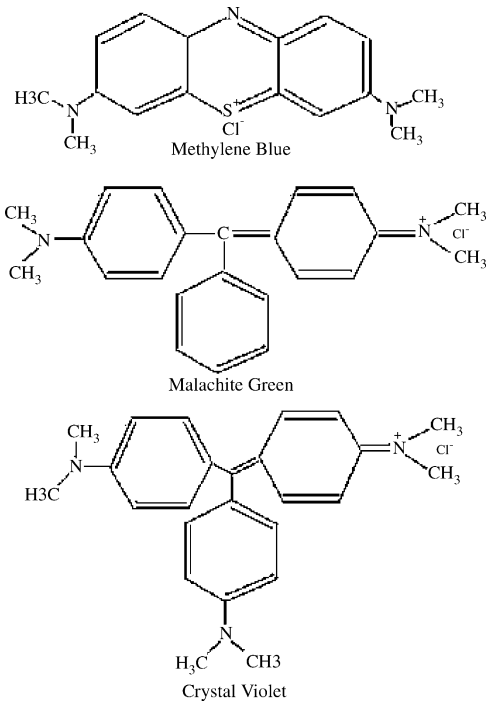

Fig. 1. Chemical structure of dyes.

parameters affecting sorption such as initial dye concentration and temperature; (iv) to determine the applicability of various isotherm model (Langmiur, Freundlich, Dubinin–Redushkevich (D–R), Temkin, Frumkin, Harkins–Jura, Halsey and Henderson) based on the correlation coefficient to find out the best-fit isotherm equation.

2. Experimental

2.1. Materials

Three dyes were used in the study. Those selected dyes are regarded as dye contaminants in the discharged effluents. The dyes, methylene blue (MB), CI = 52,015, chemical formula = $C_{16}H_{18}ClN_3SH_2O$, MW = 337.85 g/mol, λ_{max} = 660 nm was supplied by Panreac; malachite green (MG), CI = 42,000, chemical formula = $C_{50}H_{52}N_4O_8$, MW = 927.03 g/mol, λ_{max} = 617 nm; crystal violet (CV), CI = 42,555, chemical formula = $C_{25}H_{30}ClN_3$, MW = 407.99 g/mol, λ_{max} = 594 nm were supplied by Merck (1398). Chemical structures of the selected dyes are given in Fig. 1. 2000 mg/L stock solution was prepared by dissolving the required amount of dye in double distilled water. Working solutions of the desired concentrations were obtained by successive dilutions.

2.2. Preparation of activated carbon (WA11Zn5)

Brought containers, waste apricot supplied by Malatya apricot plant were dried under laboratory conditions and then dried again at 100 °C (Model FN 400, Nüve) until it reaches a constant weight. Starting material was stored in plastic tubes after grounding.

In the first step of activation, the starting material was mixed with $ZnCl_2$ at the $ZnCl_2$/starting material weight ratio of 1:1 and the mixture was kneaded with adding destile water. The mixture was then dried at 110 °C to prepare the impregnated sample.

In the second step, the impregnated sample was placed on a quartz dish, which was then inserted in a quartz tube (i.d. = 60 mm). The impregnated sample was heated up to activation temperature (500 °C) under N_2 flow (100 ml min^{-1}) at the rate of 10 °C min^{-1} and hold at the activation temperature for 1 h. After activation, the sample was cooled down under N_2 flow and 0.5N HCl was added on to activated sample. Activated sample was washed sequentially several times with hot distillated water to remove residual chemical until it did not give Cl reaction with $AgNO_3$. The washed sample was dried at 110 °C to prepare activated carbon.

2.3. Instrumentation

A Tri Star 3000 (Micromeritics, USA) surface analyzer was used to measure nitrogen adsorption isotherm at 77 K in the range of relative pressure 10^{-6} to 1. Before measurement, the sample was degassed at 300 °C for 2 h. The BET surface area, total pore volume, average pore radius, micropore area were obtained from the adsorption isotherms. Mesopore volume was determined by subtracting the micropore volume from total pore volume.

The spectrophotometric determination of dyes was done on a Shimadzu UV–vis spectrophotometer (model UV-2100S).

2.4. Adsorption experiments

To monitor the adsorption process at different temperatures (30, 40 and 50 °C) batch techniques was employed. Adsorption isotherms were recorded over the concentration range 50–400 mg/L of dye solutions in a series of 100 ml graduated conical flaks containing 50 ml solution of each concentration. A known amount (0.1 g WA11Zn5/50 ml dye solution of desired concentration) of activated carbon is then added into the solution and conical flask is stirred with thermostatic bath operating at 400 rpm. The amount of dye adsorbed onto WA11Zn5, q_t

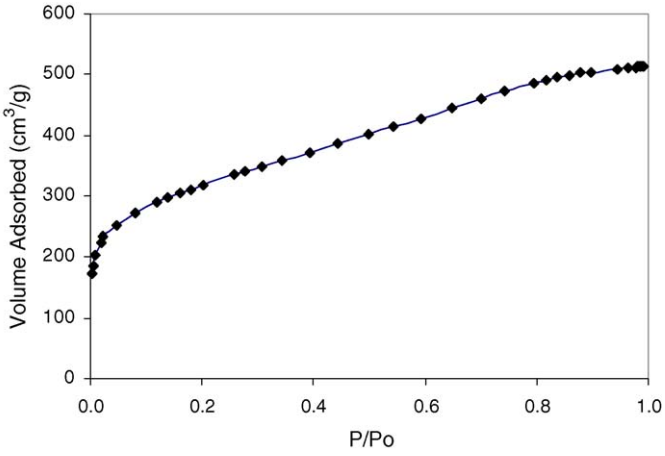

Fig. 2. Adsorption isotherm of nitrogen at 77 K for activated carbon (WA11Zn5).

Table 1
Porous structure parameters of the activated carbon (WA11Zn5)

S_{BET} (m^2/g)	S_{ext}[a]		S_{mic}		V_t	V_{mic}		V_{meso}		D_p[b]
	(m^2/g)	(%)	(m^2/g)	(%)	(cm^3/g)	(cm^3/g)	(%)	(cm^3/g)	(%)	(nm)
1060	778	74	282	36	0.79	0.15	19	0.64	81	2.98

[a] $S_{ext} = S_{meso}$.
[b] 4V/A by BET.

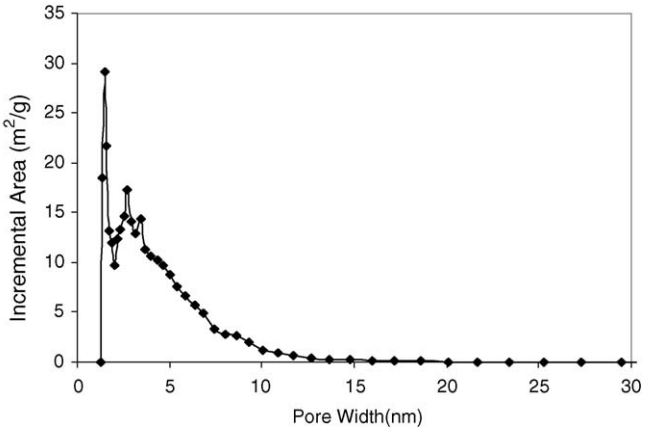

Fig. 3. Pore size distribution of the WA11Zn5.

(mg/g), was calculated by mass–balance relationship Eq. (1):

$$q_t = (C_0 - C_t)\frac{V}{W} \quad (1)$$

where C_0 and C_t are the initial and time t liquid-phase concentration of the dye (mg/L), respectively, V the volume of the solution (L) and W the weight of the dry WA11Zn5 used (g).

3. Results and discussion

3.1. Characterization of the prepared activated carbon (WA11Zn5)

Nitrogen adsorption, because the relatively small molecule diameter of nitrogen is frequently used at 77 K to probe porosity and surface area and to be a standard procedure for the characterization of porosity texture of carbonaceous adsorbents also. The adsorption isotherm is the information source about the porous structure of the adsorbent, heat of adsorption, characteristic of physical and chemical and so on. Adsorption isotherm may be grouped six types. As illustrated in Fig. 2, WA11Zn5 exhibit adsorption isotherm of type IV according to IUPAC [8]. The type IV isotherm is characteristic properties of solids having both micro and mesopores. The initial part of the isotherm follows the same path as the corresponding type II isotherm and therefore the result of monolayer–multilayer adsorption on the mesopore walls [9]. The BET surface area (S_{BET}), external surface area (including only mesopores S_{ext}), micropores surface area (S_{mic}), total pore volume (V_t) and average pore diameter (D_p) results obtained by applying the BET equation to N_2 adsorption at 77 K and DR equation to N_2 adsorption at 77 K are listed in Table 1.

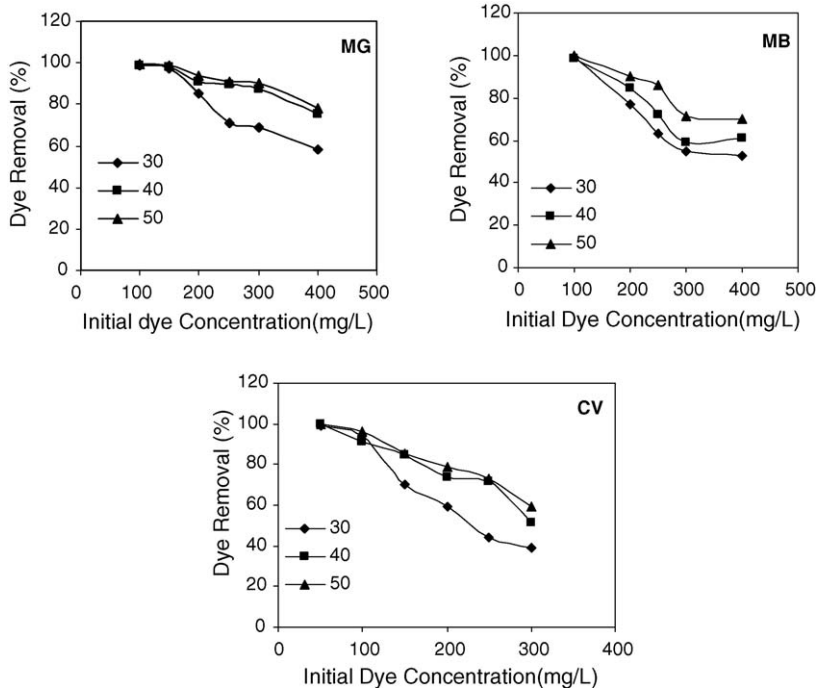

Fig. 4. Effect of initial dye concentration on the adsorption of MG, MB and CV at different temperature.

Fig. 3 shows the pore size distribution was calculated in the standard manner by using BJH method [10]. It appears that activated carbon includes both micro and mesopores. Percentages of micropores and mesopores area are 36% and 74%, respectively.

3.2. Effect of initial dye concentration on adsorption at different temperatures

Effect of initial dye concentration on adsorption was investigated at concentration ranging from 100 to 400 mg/L in case of MG, MB and 50 to 300 mg/L in case of CV at different temperatures (30, 40 and 50 °C). Fig. 4 illustrates the effect of initial dye concentration on adsorption of MG, MB and CV at different temperatures. The uptake is almost 100% at low dye concentration for all temperatures and 59–79% at higher concentration at high temperatures. Furthermore, adsorption increased with an increase in temperature, indicating that the process is endothermic.

3.3. Adsorption isotherms

In order to determine the mechanism of MG, MB and CV adsorption on the activated carbon prepared waste apricot (WA11Zn5) and evaluate the relationship between adsorption temperatures, the experimental data were applied to the Langmiur, Freundlich, D–R, Temkin, Frumkin, Harkins–Jura, Halsey and Henderson isotherm equations. The constant parameters of the isotherm equations for this adsorption process were calculated by regression using linear form of the isotherm equations. The constant parameters and correlation coefficient (R) are summarized in Table 2.

Langmuir [11] proposed a theory to describe the adsorption of gas molecules onto metal surfaces. The Langmuir adsorption isotherm has been successfully applied to many real sorption

Table 2
Constant parameters and correlation coefficients calculated for various adsorption models at different temperatures for MB, MG and CV

	MB			MG			CV		
Isotherm equations	30 °C	40 °C	50 °C	30 °C	40 °C	50 °C	30 °C	40 °C	50 °C
Langmiur									
Q_0 (mg/g)	102.04	113.64	136.98	116.27	158.73	163.93	57.80	80.0	91.74
b (L/mg)	0.072	0.093	0.123	0.123	0.140	0.176	0.673	0.377	0.227
R^2	0.950	0.935	0.958	0.983	0.985	0.987	0.998	0.989	0.993
Freundlich									
k_f (L/g)	47.99	47.73	56.48	50.41	51.92	70.91	31.20	31.89	34.292
n	8.00	6.34	5.89	6.44	4.30	6.22	7.56	4.89	4.68
R^2	0.904	0.906	0.958	0.906	0.961	0.948	0.885	0.954	0.987
D–R									
$q_m \times 10^4$ (mol/g)	3.78	4.86	5.96	2.00	3.67	3.87	2.18	3.68	4.20
$K' \times 10^4$ (mol^2/kJ^2)	10	11	11	11	15	14	10	13	13
E (kJ/mol)	22.36	21.32	21..32	21.32	18.25	18.89	22.36	19.61	19..61
R^2	0.886	0.901	0.946	0.911	0.959	0.967	0.925	0.949	0.987
Temkin									
B_1	8.67	11.79	13.85	12.05	21.18	21.47	5.24	9.84	10.96
K_T (L/mg)	211.64	45.86	63.99	50.84	8.88	12.40	514.66	31.82	28.99
R^2	0.813	0.815	0.883	0.910	0.938	0.944	0.92	0.882	0.957
Frumkin									
a	1.42	1.11	0.994	0.93	0.72	0.71	0.96	0.88	0.82
$\ln k$	6.47	6.55	6.45	7.61	7.15	7.10	7.52	7.10	6.95
$-\Delta G$	16.3	17.1	17.4	19.17	18.61	19.06	18.96	18.47	18.66
R^2	0.948	0.966	0.973	0.987	0.995	0.996	0.987	0.987	0.997
Harkins–Jura									
A	10×10^3	5×10^3	10×10^3	10×10^3	5×10^3	10×10^3	2×10^3	1.7×10^3	2×10^3
B	4.00	2.00	3.00	4.00	1.50	1.50	2.40	2.04	2.20
R^2	0.977	0.957	0.969	0.799	0.856	0.858	0.807	0.927	0.884
Halsey									
n	7.99	6.32	5.90	6.44	4.30	4.31	7.56	4.89	4.68
k	2.74×10^{13}	4.06×10^{10}	2.20×10^{10}	9.54×10^{10}	2.42×10^7	3.65×10^7	2×10^{11}	2.26×10^7	1.53×10^7
R^2	0.903	0.907	0.958	0.906	0.961	0.968	0.885	0.950	0.985
Henderson									
n	7.35	5.83	5.71	5.93	4.17	4.21	6.77	4.68	4.65
k	6.2×10^{-16}	2.3×10^{-13}	1.13×1^{-13}	1.1×10^{-13}	4.5×10^{-11}	7.64×10^{-11}	1.1×10^{-13}	1.1×10^{-10}	7.6×10^{-11}
R^2	0.907	0.909	0.958	0.905	0.960	0.968	0.881	0.947	0.984

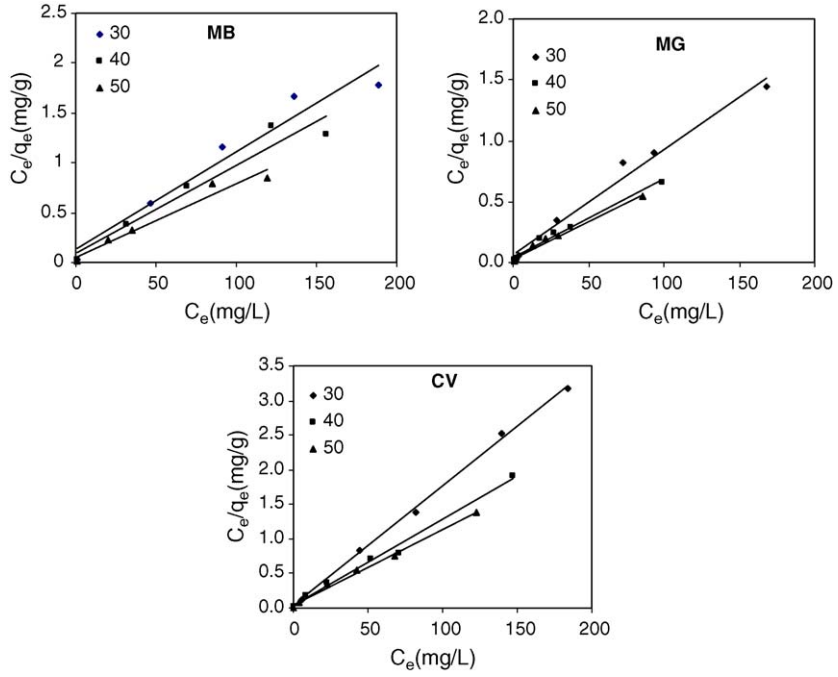

Fig. 5. Langmuir isotherm plots for the removal of MB, MG and CV (temperature = 30, 40, 50 °C, contact time = 60 min).

processes. The linearized Langmuir isotherms is represented by following equation:

$$\frac{C_e}{q_e} = \frac{1}{Q_0 b} + \frac{C_e}{Q_0} \quad (2)$$

where C_e is the dye concentration at equilibrium (mg/L), q_e the adsorption capacity in equilibrium (mg/g), b the Langmuir adsorption constant (L/mg), and Q_0 is the signifies adsorption capacity(mg/g). Fig. 5 shows the Langmuir (C_e/q_e versus C_e) plots for the removal of MG, MB and CV at different temperatures. The isotherms of all three dyes, namely MB, MG and CV were found to be linear over the whole concentration range studies and the correlation coefficients were extremely high as shown in Table 2. The value of Q_0 increases with temperature increase,

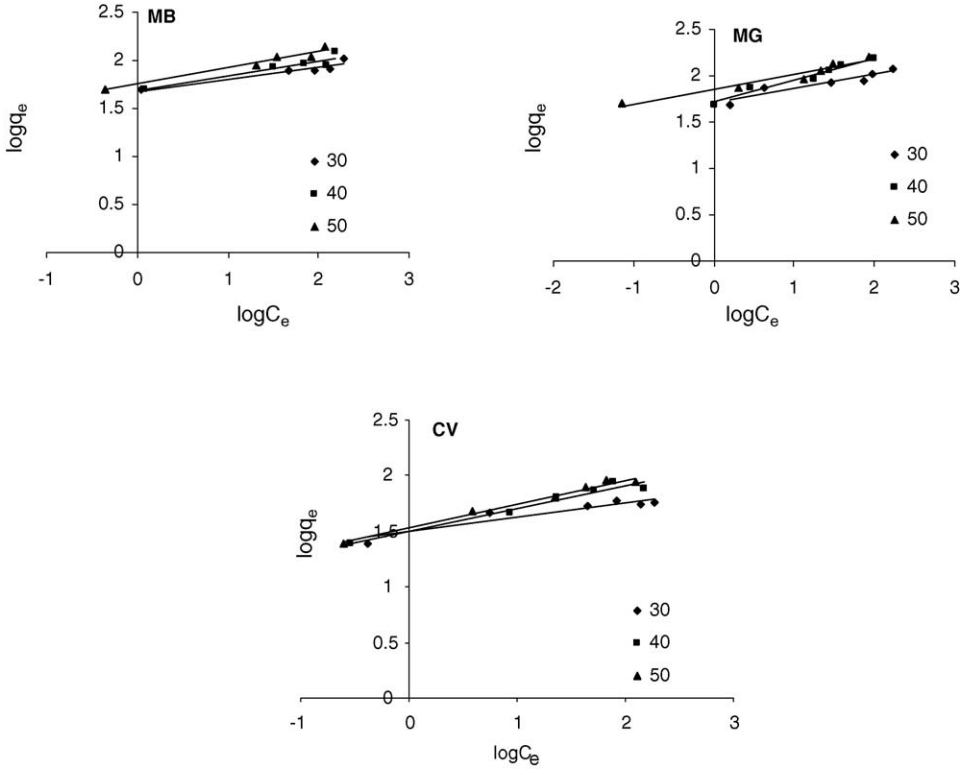

Fig. 6. Freundlich isotherm plots for the removal of MB, MG and CV (temperature = 30, 40, 50 °C, contact time = 60 min).

thereby confirming that the process is endothermic [12,13]. The value of Q_0 is significantly higher for the MG-WA11Zn5 system compared to MB and CV on the same adsorbent. At 50 °C, the maximum adsorption capacities were determined as 136.98 mg/g for MB, 163.93 mg/g for MG, 91.74 mg/g for CV. To determine if adsorption process is favorable or unfavorable, for the Langmuir type adsorption process, isotherm can be classified by a term 'R_L', a dimensionless constant separation factor, which is defined as below [14].

$$R_L = \frac{1}{(1 + bC_0)} \tag{3}$$

The R_L values are found in the range of 0.02–0.12, 0.014–0.075 and 0.0049–0.089 for MB, MG and CV at 30, 40 and 50 °C, respectively, showing favorable adsorption.

The Freundlich adsorption isotherm can be expressed [15] as

$$\log q_e = \log k_f + \frac{1}{n} \log C_e \tag{4}$$

where k_f (L/g) and n are isotherm constant which indicate the capacity and intensity of the adsorption, respectively. The linear plot of $\log q_e$ versus $\log C_e$ at each temperature indicates that adsorption of MG, MB and CV also follows Freundlich isotherm (Fig. 6). Table 2 shows the Freundlich adsorption isotherm constant and correlation coefficients. The values of k_f and n determined from the Freundlich model changed with the rise in temperature. The value of n for Freundlich isotherm was found to be greater than 1, indicating that MB, MG and CV dyes are favorably adsorbed by WA11Zn5 at all the temperatures studied [16,17].

The D–R equation can be expressed [18] as

$$q_e = q'_m \exp(-K'\varepsilon^2) \tag{5}$$

where ε (Polanyi potential) is equal to $RT\ln(1 + 1/C_e)$, q_e is the amount of the dye adsorbed per unit activated carbon (mol/g), q_m the theoretical monolayer saturation capacity (mol/g), C_e the equilibrium concentration of the dye solution (mol/L), K' the constant of the adsorption energy (mol^2/kJ^2), R the gas constant (kJ/mol K), and T is the temperature (K). The linear form of the D–R isotherm is

$$\ln q_e = \ln q_m - K'\varepsilon^2 \tag{6}$$

K' is related to mean adsorption energy (E, kJ/mol) as [19]

$$E = \frac{1}{\sqrt{2K'}} \tag{7}$$

The plot of $\ln q_e$ versus ε^2 at 30, 40, 50 °C adsorption temperature is presented in Fig. 7. The constant obtained for D–R isotherms are shown in Table 2. The mean adsorption energy (E) gives information about chemical and physical adsorption [20]. It was found to be in the range of 18.25–22.36 kJ/mol, which is bigger then the energy range of adsorption reaction, 8–16 kJ/mol. The type of adsorption of MB, MG and CV on the WA11Zn5 was defined as chemical adsorption [21].

Heat of adsorption and the adsorbate–adsorbate interaction on adsorption isotherms were studied by Temkin and Pyzhev [22]. The Temkin isotherm equation is given as

$$q_e = \frac{RT}{b} \ln(K_T C_e) \tag{8}$$

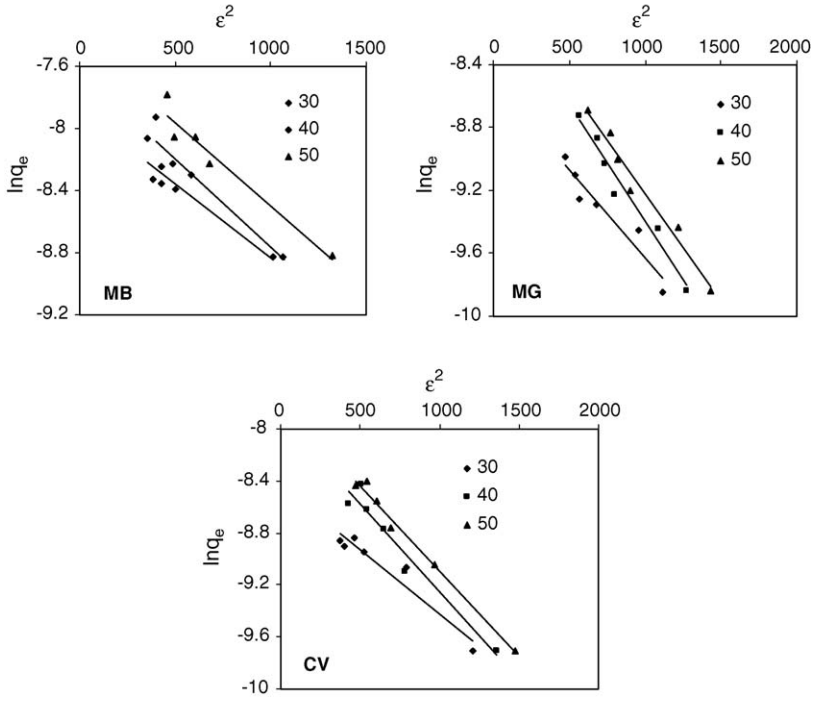

Fig. 7. D–R adsorption isotherm for MB, MG and CV at different adsorption temperature.

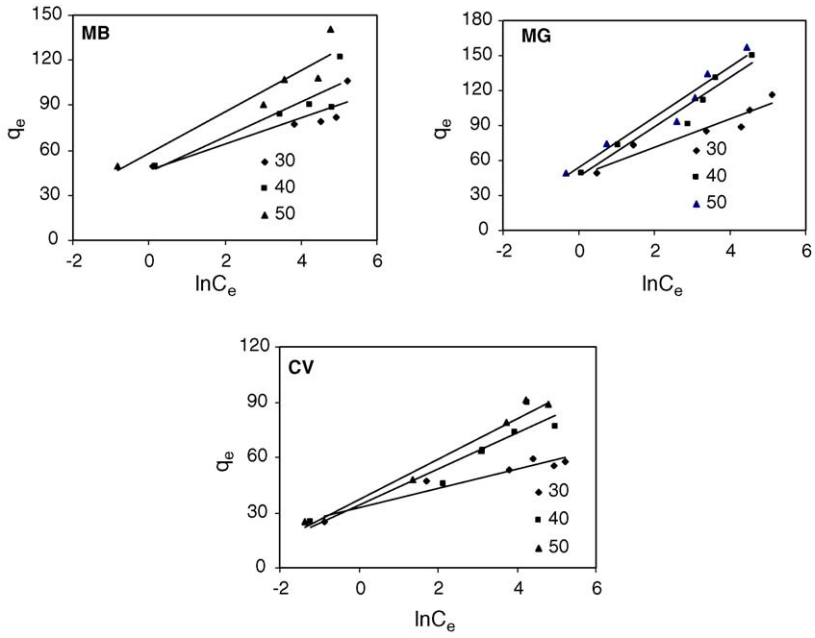

Fig. 8. Temkin isotherm for MB, MG and CV at different adsorption temperature.

Eq. (8) can be linearized as

$$q_e = B_1 \ln K_T + B_1 \ln C_e \quad (9)$$

where $B_1 = RT/b$, T is the absolute temperature in K, R the universal gas constant, 8.314 J/mol K_T the equilibrium binding constant (L/mg) and B_1 is related to the heat of adsorption. A plot q_e versus $\ln C_e$ at studied temperature is given in Fig. 8. The constant obtained for Temkin isotherms are shown in Table 2. The Temkin isotherm constant in Table 2 shows that the heat of adsorption (B_1) increases with increase in temperature, indicating endothermic adsorption [23].

Frumkin isotherm, which takes into account interaction between the adsorbed species [24]. The Frumkin adsorption isotherm can be expressed as

$$\frac{\theta}{1-\theta} e^{-2a\theta} = kC_e \quad (10)$$

where θ is the fractional occupation ($\theta = q_e/q_m$; q_e is the adsorption capacity in equilibrium (mg/g), q_m the theoretical monolayer saturation capacity (mg/g) which is determined by D–R isotherm equation), and C_e is the concentration of dye on the

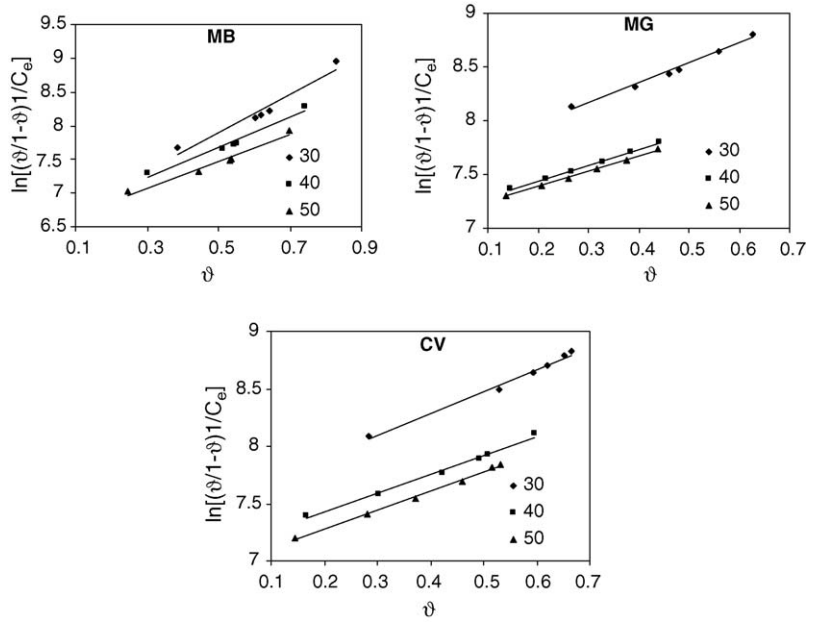

Fig. 9. Frumkin isotherm for MB, MG and CV at different adsorption temperature.

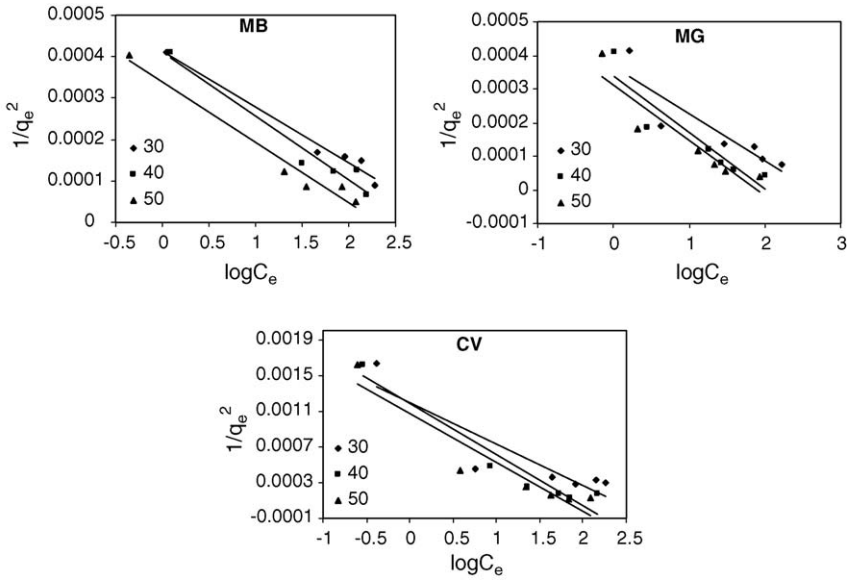

Fig. 10. Harkins–Jura isotherm for MB, MG and CV at different adsorption temperature.

adsorbent at equilibrium (mol/L). In the linearized form

$$\ln\left[\left(\frac{\theta}{1-\theta}\right)\frac{1}{C_e}\right] = \ln k + 2a\theta \tag{11}$$

The parameters a and k are obtained from slope and intercept of the plot $\ln\left[\left(\frac{\theta}{1-\theta}\right)\frac{1}{C_e}\right]$ versus θ. The constant k is related to adsorption equilibrium.

$$\ln k = \frac{-\Delta G}{RT} \tag{12}$$

The parameter a is the interaction coefficient, it is positive for attraction and negative for repulsion; its zero value indicates no interaction between the adsorbate species in which case the Frumkin equation coincides with Langmiur one [25]. The plot $\ln\left[\left(\frac{\theta}{1-\theta}\right)\frac{1}{C_e}\right]$ versus θ at studied temperature is given in Fig. 9. Frumkin isotherm constants are summarized in Table 2. The positive a values indicate that there is attractive interaction between the adsorbed species [26]. The different a values are attributed to differences in the orientation of the dye molecules. In general trend, attractive interaction decreases with increasing temperature. The ΔG^0 values varied in a narrow range with the mean values −16.9, −18.94, −18.69 kJ/mol for adsorption of MB, MG and CV, respectively, in accordance with the endothermic nature of the adsorption process [18,27].

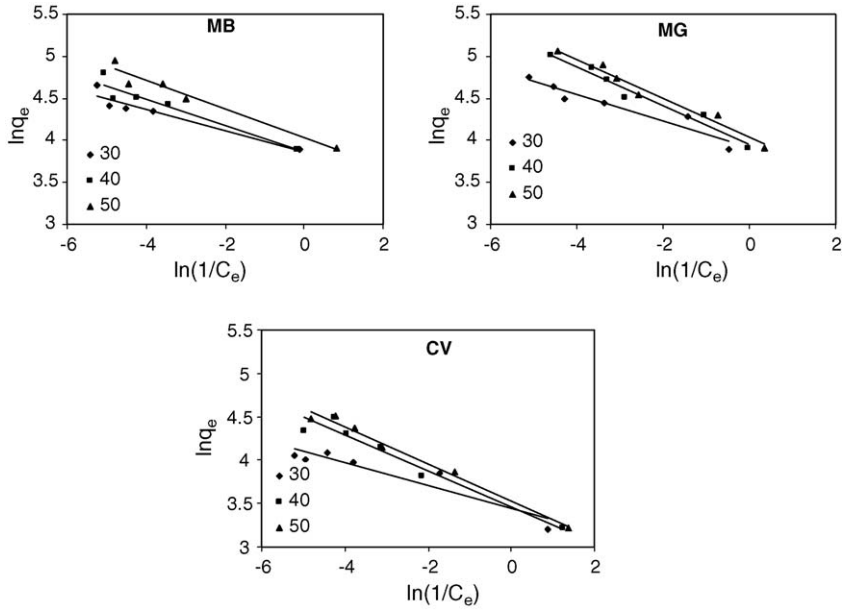

Fig. 11. Halsey isotherm for MB, MG and CV at different adsorption temperature.

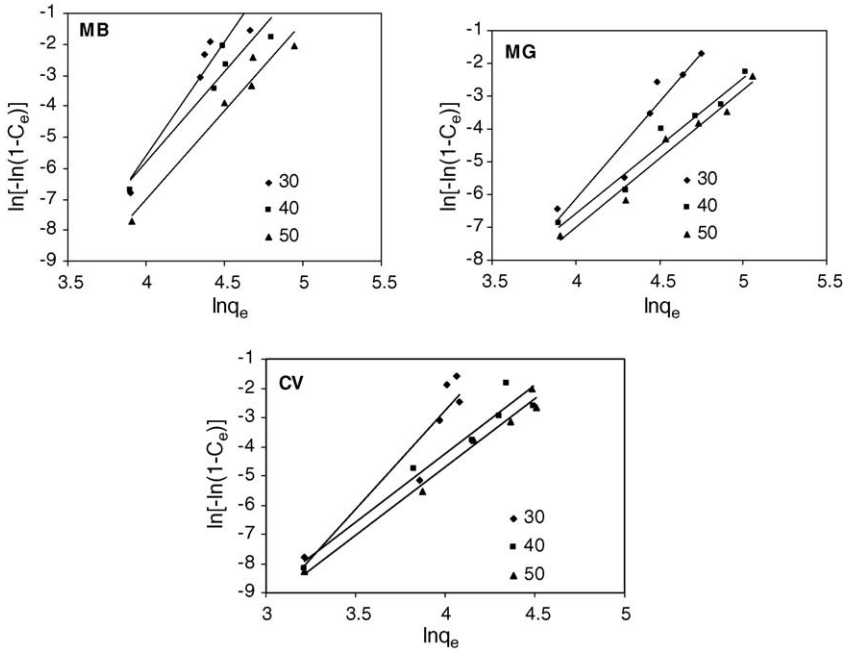

Fig. 12. Handerson isotherm for MB, MG and CV at different adsorption temperature.

The Harkins–Jura adsorption isotherm can be expressed [28] as

$$\frac{1}{q_e^2} = \left(\frac{B}{A}\right) - \left(\frac{1}{A}\right) \log C_e \quad (13)$$

which accounts to multilayer adsorption can be explained with the existence of a heterogeneous pore distribution. $\frac{1}{q_e^2}$ versus $\log C_e$ Harkins–Jura isotherms are given in Fig. 10. Isotherm constants and correlation coefficients are summarized in Table 2.

Halsey [29] and Henderson [30] adsorption isotherm can be given as, respectively,

$$\ln q_e = \left[\left(\frac{1}{n}\right) \ln k\right] - \left(\frac{1}{n}\right) \ln C_e \quad (14)$$

$$\ln[-\ln(1 - C_e)] = \ln k + n \ln q_e \quad (15)$$

These equations are suitable for multilayer adsorption. Especially, the fitting of these equations can be heteroporous solids [31] $\ln q_e$ versus $\ln C_e$ Halsey and $\ln[-\ln(1 - C_e)]$ versus $\ln q_e$ Henderson adsorption isotherms are given in Figs. 11 and 12, respectively. Isotherm constants and correlation coefficients are summarized in Table 2. The constant n values of Halsey and Henderson equation decrease with increasing temperature, which show that adsorption increased with a decrease in n values, indicating that the process is endothermic [32].

4. Conclusions

The results of this work can be summarized as follows:

(1) The N_2 adsorption isotherm of WA11Zn5 is of type IV. The values of S_{BET}, V_t, S_{mic}, V_{mic}, S_{meso}, and V_{meso} are 1060 m^2/g, 0.79 cm^3/g, 282 m^2/g, 0.15 cm^3/g, 778 m^2/g, and 0.64 cm^3/g, respectively. Results show that activated carbon includes micropores and mesopores. Percentage of micropores and mesopores area is 36% and 74%, percentage of micropores and mesopores volume is 19% and 81%, respectively.

(2) The adsorption capacities of WA11Zn5 decreases in the order malachite green (MG) > methylene blue (MB) > crystal violet (CV). The amount of dye adsorbed onto WA11Zn5 for 400 mg/L initial dye concentration are 116, 150, 157 mg/g (for MG), 105, 122, 140 mg/g (for MB), 58, 77, 89 mg/g (for CV) at 30, 40, 50 °C, respectively. Adsorption of all dyes onto WA11Zn5 increased with an increase in temperature, indicating that the process is endothermic.

(3) Langmiur, Freundlich, Dubinin–Redushkevich (D–R), Temkin, Frumkin, Harkins–Jura, Halsey and Henderson equation were used to describe the adsorption of MG, MB and CV onto WA11Zn5. Langmiur and Frumkin model have better correlation coefficient than the other model in the studied concentration at all temperatures studied, generally. But Harkins–Jura model has high correlation coefficient for adsorption of MB onto WA11Zn5 at all temperatures.

(4) The adsorption of the dyes, MG, MB and CV, was found to be endothermic according to Langmuir, Frumkin isotherms. R_L separation factor for Langmuir show that the MG, MB and CV are favorably adsorbed by activated carbons prepared from waste apricot. The negative values of Gibbs free energies (ΔG) calculated from Frumkin constant (k) at all temperatures, indicating that the process of MG, MB and CV adsorption is favored at high temperatures.

References

[1] M. Clark Robert, Granular Activated Carbon Design, Operation, and Cost, Lewis Publishers, 1989.
[2] AWWA, Handbook of Water Supplies, vol. 439, McGraw Hill, 1971.
[3] R. Han, J. Zhang, W. Zou, J. Shi, H. Liu, J. Hazard. Mater. 125 (2005) 266–271.
[4] D. Güzey, M. Özdemir, F.G. Seyhan, H. Doğan, Y.O. Devres, Drying Tech. 19 (2001) 691–699.
[5] R.C. Wang, C.C. Kuo, C.C. Shyu, J. Chem. Tech. Biotechnol. 68 (1997) 187–194.
[6] Z. Aksu, Ö. Tunç, Process Biochem. 40 (2005) 831–847.
[7] S. Karaca, A. Gürses, M. Ejder, M. Açıkyıldız, J. Hazard. Mater., in press.
[8] K.W. Sing, D.H. Everet, R.A.W. Haul, L. Moscou, R.A. Pierotti, J. Rouquero, T. Siemieniewasa, Pure Appl. Chem. 57 (1985) 603.
[9] Z. Ryu, J. Zheng, M. Wang, B. Zhang, Carbon 37 (1999) 1257.
[10] P.E.P. Barrett, L.G. Joyner, P.P. Halenda, J. Am. Chem. Soc. 73 (1951) 373.
[11] I. Langmuir, J. Am. Chem. Soc. 40 (1918) 1361.
[12] M. Ajmal, R.A.K. Rao, R. Ahmad, J. Ahmad, J. Hazard. Mater. B79 (2000) 117.
[13] V.K. Gupta, A. Mittal, V. Gajbe, Colloid Interface Sci. 284 (2005) 89.
[14] T.W. Weber, R.K. Chakkravorti, Am. Inst. Chem. Eng. J. 20 (1974) 228.
[15] H.M.F. Freundlich, Z. Physc. Chem. 57 (1906) 385.
[16] S.D. Faust, O.M. Aly, Adsorption Processes for Water Treatment, Butterworths, 1987.
[17] P.K. Malik, Dyes Pigments 56 (2003) 239.
[18] B. Acemioğlu, J. Colloid Interface Sci. 274 (2004) 371.
[19] J.P. Hobson, J. Phys. Chem. 73 (1969) 2720.
[20] W. Riemam, H. Walton, Ion exchange in analytical chemistry, International Series of Monographsin Analytical Chemistry, vol. 38, Pergamon Press, Oxford, 1970.
[21] E. Oguz, Colloid Surf. 252 (2005) 121.
[22] M.J. Temkin, V. Pyzhev, Acta Physiol. Chem. USSR 12 (1940) 271.
[23] M. Sekar, V. Sakthi, S. Rengaraj, Colloid Interface Sci. 279 (2004) 307.
[24] R. Parson, Elektrokhimiya 37 (6) (2001) 647.
[25] A. Kilislioğlu, Appl. Radiat. Isot. 58 (2003) 713.
[26] C. Quan, G. Khoe, D. Bagster, Water Res. 35 (2001) 478.
[27] Y. Önal, C. Akmil-Başar, J. Hazard. Mater., in press.
[28] W.D. Harkins, G. Jura, J. Chem. Phys. 66 (1944) 73.
[29] G. Halsey, J. Chem. Phys. 16 (1948) 931.
[30] S.M. Henderson, Agric. Eng. 33 (1952) 29.
[31] M.J. Rosen, Surfactants and Interfacial Phenomena, John Willey, New York, 1978, 32–76.
[32] MF. Ertugay, M. Certel, A. Gürses, J. Sci. Food Agric. 80 (2000) 2001.